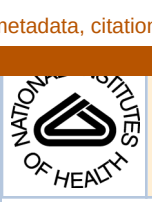

Published in final edited form as:

NMR Biomed. 2013 January ; 26(1): 98–105. doi:10.1002/nbm.2824.

^{31}P and ^{1}H MRS of DB-1 Melanoma Xenografts: Lonidamine Selectively Decreases Tumor Intracellular pH and Energy Status and Sensitizes Tumors to Melphalan

Kavindra Nath[1], **David S. Nelson**[1], **Andrew Ho**[1], **Seung-Cheol Lee**[1], **Moses M. Darpolor**[1], **Stephen Pickup**[1], **Rong Zhou**[1], **Daniel F. Heitjan**[2], **Dennis B. Leeper**[3], and **Jerry D. Glickson**[1]

[1]Department of Radiology, University of Pennsylvania

[2]Department of Biostatistics & Epidemiology, University of Pennsylvania

[3]Department of Radiation Oncology, Thomas Jefferson University, Philadelphia, Pennsylvania, USA

Abstract

In vivo ^{31}P MRS demonstrates that human melanoma xenografts in immunosuppressed mice treated with lonidamine (LND, 100 mg/kg, i.p.) exhibit a decrease in intracellular pH (pHi) from 6.90 ± 0.05 to 6.33 ± 0.10 ($p < 0.001$), a slight decrease in extracellular pH (pHe) from 7.00 ± 0.04 to 6.80 ± 0.07 ($p > 0.05$), and a monotonic decline in bioenergetics (NTP/Pi) by 66.8 ± 5.7% ($p < 0.001$) relative to the baseline level. Both bioenergetics and pHi decreases were sustained for at least 3 hr following LND treatment. Liver exhibited a transient intracellular acidification by 0.2 ± 0.1 pH units ($p > 0.05$) at 20 min post-LND with no significant change in pHe and a small transient decrease in bioenergetics, 32.9 ± 10.6 % ($p > 0.05$), at 40 min post-LND. No changes in pHi or ATP/Pi were detected in the brain (pHi, bioenergetics; $p > 0.1$) or skeletal muscle (pHi, pHe, bioenergetics; $p > 0.1$) for at least 120 min post-LND. Steady-state tumor lactate monitored by ^{1}H MRS with a selective multiquantum pulse sequence with Hadamard localization increased ~3-fold ($p = 0.009$). Treatment with LND increased systemic melanoma response to melphalan (LPAM; 7.5 mg/kg, i.v.) producing a growth delay of 19.9 ± 2.0 d (tumor doubling time = 6.15 ± 0.31d, log10 cell-kill = 0.975 ± 0.110, cell-kill = 89.4 ± 2.2%) compared to LND alone of 1.1 ± 0.1 d and LPAM alone of 4.0 ± 0.0 d. The study demonstrates that the effects of LND on tumor pHi and bioenergetics may sensitize melanoma to pH-dependent therapeutics such as chemotherapy with alkylating agents or hyperthermia.

Keywords

Phosphorus-31 MRS; Lonidamine; Monocarboxylate transporter; Tumor acidification; Melphalan; Melanoma

Introduction

Melanoma, the deadliest skin cancer (1) is the most rapidly increasing form of human cancer among Caucasian populations in the world (2). Presently, melanoma is primarily treated by surgical excision, which is often curative if the tumor is detected in its early stages. However, if recurrence occurs with metastasis, the prognosis is very poor since effective

Corresponding Address: Jerry D. Glickson, Ph.D., Professor and Director of Molecular Imaging, Department of Radiology, B6 Blockley Hall, 423 Guardian Drive, University of Pennsylvania, Philadelphia, PA 19104-6069, glickson@mail.med.upenn.edu.

methods for treating systemic disease are not available. Limited success has been achieved with agents that target the V600D, E, K, BRAF mutation observed in about 50% of melanomas (3, 4) and with Ipilumimab (5, 6) but none of these have been curative. The most promising approach for systemic treatment of this disease will probably be the development of multiple therapeutic agents functioning by a variety of independent mechanisms that would be very difficult to simultaneously circumvent. The present study demonstrates one such method that utilizes the Warburg effect and agents that trap lactate in tumors to selectively acidify melanoma and sensitize it to systemic therapy with conventional alkylating agents.

Intracellular acidification has been reported to potentiate tumor response to hyperthermia (7–9) as well as to chemotherapy with platinum (10) and N-mustard (11–13) alkylating agents. In preliminary studies of mice bearing subcutaneously implanted human DB-1 melanoma xenografts, we have achieved about 40 minutes of selective acidification of these tumors to a pHi of 6.2± 0.2 by administering high levels of exogenous glucose together with an inhibitor of oxidative phosphorylation, meta-iodobenzylguanidine (MIBG) and an inhibitor of the monocarboxylic acid transporter (MCT) (14)α-cyano-4-hydroxycinnamate (CHC) to block export of lactic acid from the tumor cells (15). Tumor acidification was accompanied by a decrease in the bioenergetic status of the tumor (NTP/Pi) by about 50%. A similar procedure was also conducted on a nude rat model of human melanoma xenografts that were treated with melphalan (LPAM) during isolated limb perfusion; local acidification was induced by administering glucose by intravenous infusion (26 mM) plus MIBG (22.5 mg/kg); subsequent infusion of LPAM produced a 51 day growth delay, whereas LPAM administered without glucose and MIBG produced only a 21 day growth delay (16).

These preliminary results could not be translated into the clinic, however, because CHC is not FDA approved, and MIBG is only approved for human use at tracer concentrations suitable for treatment with the radio-iodinated drug. Therefore, we performed studies with the putative MCT inhibitor lonidamine (LND), which has been widely used in Europe and Canada. This agent acidified the tumor under hyperglycemic conditions (26 mM blood glucose) for over 3 hr and also dramatically decreased NTP/Pi, but the animals died after the experiments were completed.

The goals of the present study were to set the stage for clinical translation by developing a treatment procedure that is reproducibly effective and produces selective acute acidification of the DB-1 melanoma with minimal toxicity to the host. There is also continuing controversy over the mechanism of action of LND that we sought to resolve. Finally, since acute acidification has been reported to enhance the activity of platinum compounds (10) and alkylating agents such as nitrogen (N)-mustards (10–13, 16–19), we have evaluated the effect of LND-induced acidification on one representative agent, LPAM. We found that while LND alone had no significant effect on tumor growth delay, it substantially enhanced the activity of LPAM and did not substantially increase the toxicity of this antineoplastic agent. These findings point to the potential utility of nitrogen mustards and LND in the systemic treatment of disseminated melanoma.

Materials and Methods

Subjects

Fifteen tumor-bearing mice were included in the study. Of the 15 tumors studied, 7 were evaluated by nonlocalized and 8 by localized ^{31}P MRS. Mice without tumors were employed in studies of normal tissues, brain pHi (n = 3), surgically exposed liver pHi (n = 6), pHe (n = 3) and skeletal muscle pHi (n = 6), pHe (n = 3), under identical conditions

utilized for ^{31}P MRS studies of mice with tumors. Three tumor-bearing mice were included for lactate measurement experiments following LND administration.

Materials

LND and 3-aminopropylphosphonate (3-APP) were purchased from Santa Cruz Biotechnology, Inc (Santa Cruz, CA, USA). The drug (LND; 5 mg) was dissolved in 227 μL of tris/glycine buffer (22.0 mg/mL), vortexed until the solution was clear and administered i.p. (intraperitoneal) at a dose of 100 mg/kg. The buffer consisted of trizma base (1.2 g) and glycine (5.76 g) in 100 mL sterile water (final pH = 8.3). In addition, 0.2 ml of a 300 mg/ml solution of 3-APP (dissolved in water and pH adjusted to 7) was administered i.p. LPAM was purchased from Santa Cruz Biotechnology, Inc (Santa Cruz, CA, USA) and was dissolved by solubilization in 5% acid (HCl)/ethanol at 15 mg/ml followed by 10-fold dilution with PBS (1.5 mg/ml) immediately prior to i.v. administration (7.5 mg/kg).

Human Melanoma Xenografts in Nude Mice

Male athymic nude mice (01B74) 4–6 weeks of age obtained from the National Cancer Institute, Frederick, MD, USA were housed in microisolator cages and had access to water and autoclaved mouse chow *ad libitum*. DB-1 melanoma cells were obtained and preserved as discussed before (14). Cells expressed human melanoma antigens (20). DB-1 cells were grown as monolayers at 37°C in 5% CO2 in α-MEM (Invitrogen/Gibco, Carlsbad, CA, USA) supplemented with 10% fetal calf serum, 1% glutamine, HEPES, penicillin, streptomycin and glucose (2.5 M). One million melanoma cells in 0.10 mL of Hank's balanced salt solution (Invitrogen/Gibco, Carlsbad, CA, USA) were inoculated subcutaneously into the right thigh of each animal. Melanoma xenografts were allowed to grow until the tumor volume reached ~300 mm^3 before further study. The tumor dimensions were measured with calipers in three orthogonal directions, and the volume was calculated using the equation, $V = \pi(a \times b \times c)/6$, where a, b, and c are the length, width, and depth of the tumor.

Animal Preparation

For induction of anesthesia, tumor-bearing mice were administered an i.p. cocktail containing ketamine hydrochloride (10 mg/mL) and acepromazine (1 mg/mL) with the total dose equivalent to 50 mg/kg ketamine and 5 mg/kg. Once positioned for study, animals were maintained under 1% isoflurane in oxygen, supplied at 1 L/min. Changes in pHi and pHe in response to LND were monitored in tumor, brain, skeletal muscle, and exposed liver of nude mice. Tumor, skeletal muscle (hind-leg) and exposed liver were studied by positioning the tissue in a home-built dual-frequency (^{1}H/^{31}P) slotted-tube resonator (13 mm in diameter). Brain ^{31}P MRS was implemented by placing the animal's head on top of a 20 mm ^{31}P surface coil in conjunction with a 70 mm quadrature ^{1}H volume coil (T/R). For ^{31}P MRS experiments on liver, a 1-cm incision was made in the abdomen of the anesthetized animal to expose the liver, and the exposed organ was placed inside the resonator. During the liver studies some surface dehydration was evident in the surgically exposed liver; this produced some discoloration of the liver surface and small modifications of the ^{31}P spectrum. Both effects of dehydration were eliminated by placement of a parafilm insert filled with saline inside the resonator to maintain hydration of the tissue. For lactate measurements following LND administration, tumors were positioned in a home-built single frequency (^{1}H) slotted tube resonator (inner diameter = 13 mm, outer diameter = 15 mm, depth = 16.5 mm).

MR Experiment and pH Estimation

MR experiments were performed on a 9.4 T/31 cm horizontal bore Varian system. *In vivo* ^{31}P MR spectra were acquired with a homemade resonator as described above. Sub-

dermal needle electrodes and a rectal thermistor were placed for electrocardiogram and core body temperature monitoring, respectively. The animal's core body temperature was maintained at 37 ± 1°C by blowing warmed air into the bore of the magnet during a scan with heating controlled by a thermal regulator system. A respiration pillow was placed over the thorax and a pulse-oximeter over the tail to monitor respiration and oxygen saturation, respectively (Model 1025, SA Instruments Inc., Stony Brook, NY, USA). For measurement of pH_e (21), LND and 3-APP were injected following acquisition of the baseline spectrum through two 26 gauge i.p. catheters inserted into either side of the peritoneum without removing the animal from the magnet. The magnet was shimmed until the water line-width of the tumor monitored via the ^{1}H channel reached 60–70 Hz. Nonlocalized ^{31}P MRS experiments were performed using the following parameters: 128 scans (NT) with an rf pulse width of 60 μs, corresponding approximately to a 90° flip angle; 12 kHz sweep width (SW); 512 data points (NP); TR of 4 sec. Localized ^{31}P MRS was performed on tumor (n=8) and brain (n=3) using the ISIS (Image Selected *In vivo* Spectroscopy) technique with the following parameters: NT = 256 with an rf pulse width of 60 μs, corresponding approximately to a 90° flip angle; SW =12 kHz; NP = 512; TR of 4 sec. In order to permit simultaneous measurement of pHi, pHe and NTP/Pi ratios in single ^{31}P MRS spectra, we chose to use the pHe indicator 3-APP rather than a ^{1}H detectable probe (22), which could have provided higher spatial resolution. The localization method (ISIS) requires calibration of pulse parameters that is very demanding and time consuming. When we did, we found that the results obtained with ISIS localization were consistent with the nonlocalized spectra. A PRESS (Point Resolved Spectroscopy) sequence was used to shim the ISIS tumor voxel, as well as the voxel localized studies of the brain. A slice selective double frequency Hadamard Selective Multiple Quantum Coherence (Had-Sel-MQC) pulse sequence was used to detect lactate and to filter out overlapping lipid signals (23). The acquisition parameters were: SW = 4 kHz, NP = 2048, TR = 8 s, NT = 128. NUTS (Acorn NMR Inc., Livermore, CA, USA) and MestRec (Mestrelab Research, Santiago de Compostela, Spain) were used to process all spectroscopic data. A 20 Hz exponential filter was used to improve the apparent signal-to-noise ratio of ^{31}P MRS data, and base-line correction was applied before plotting and calculating peak areas. The pH_i was determined from the chemical shifts of Pi referenced to the α-NTP resonance.

Intracellular and extracellular pH was determined as discussed before (14). For pHe, the pKa of 6.90 ± 0.03, limiting acid chemical shift of 34.22 ± 0.04 ppm, and base chemical shift of 31.08 ± 0.04 ppm were used, and for pHi, the corresponding parameters were 6.57 ± 0.03, 13.52 ± 0.03, and 11.24 ± 0.02 ppm, respectively (14, 24–26). For each animal, the change in NTP/Pi (bioenergetics status) relative to its baseline value was determined after LND administration.

Treatment with Chemotherapy and Tumor Volume Measurement

When tumors reached ~250 mm^3 in volume, four cohorts of five age- and weight-matched animals were randomized to the following treatment groups: cohort 1 (sham treated control) was infused intravenously (i.v.) with PBS and given appropriate sham intraperitoneal (i.p.) injections of tris/glycine buffer; cohort 2 was infused i.v. with PBS 40 minutes after LND administration i.p. (100 mg/kg); cohort 3 was injected i.p. with tris/glycine buffer and infused i.v. with LPAM (7.5 mg/kg delivered in ~10 sec) in PBS; cohort 4 was injected i.p. with LND (100 mg/kg) and after 40 minutes, LPAM (7.5 mg/kg) was infused i.v.

During the treatment and sham-treatment procedures, all animals were anesthetized with ketamine hydrochloride and acepromazine as described above with additional anesthesia being readministered as needed approximately every 45–60 min. Animals were placed on a water pad heater (Gaymar T-Pump) to maintain body temperature during anesthesia. Tumor dimensions were measured as well as animal body weight. Tail vein catheters (I.V.

Catheters FEP, Tyco Healthcare) filled with heparin (100 USP Units/mL) to prevent blood clotting were placed using a restrainer (MTI Braintree Scientific). LPAM was freshly prepared prior to injection. Depending on the treatment group, either tris/glycine or LND (4.5 ul/g) and LPAM or PBS (5.0 ul/g) were injected. Tail vein catheters were removed and animals were allowed to recover in cages.

For the first five days post-treatment, tumor volume and body weight were measured daily with calipers (Scienceware) and scale (Acculab PP-401), respectively. Afterwards, these measurements were repeated every other day.

Statistics

ANOVA with Bonferroni and Tukey multiple comparisons were used for statistical analysis (STATA® software version 12.0). The data of pHi, pHe, lactate, NTP/Pi at time points following LND administration were compared. We tested the null hypothesis versus alternative hypothesis at the significance level of $\alpha = 0.05$. To assess the significance of treatment effects, we fit spline models to the longitudinal tumor growth data (27). The models described log tumor volume as linear throughout the period of observation in the control arm and prior to treatment in the active arms, and as a quadratic spline in the period immediately after treatment in the active arms. We evaluated significance of the treatment effects by likelihood ratio tests involving the spline coefficients. We conducted the tumor growth modeling in SAS Proc Mixed (SAS Version 9.2; SAS Institute; Cary, NC). Other analyses were performed in Microsoft Excel 2010.

Results

A representative localized ^{31}P MR spectrum of human melanoma xenografts prior to administration of LND is shown in figure 1A. The corresponding spectrum following injection of LND is shown in figure 1B.

The pHi and pHe profiles of the melanoma xenografts after LND administration are plotted in figure 2A, B, respectively. The MR experiments showed a monotonic decrease in tumor pHi after LND administration (Fig. 2A). A maximum decrease in tumor pH_i of 0.6 ± 0.1 units ($p < 0.001$) was observed at 80 min following LND administration. However, the tumor pHe exhibited a smaller gradual decline by 0.2 ± 0.07 units overall ($p > 0.05$) (Fig. 2B). The pHi and pHe changes in normal tissues (liver, skeletal muscle, and brain) in response to LND administration are summarized in figure 2A, B, respectively. The surgically exposed liver showed a small transient decrease in pHi of 0.2 ± 0.1 units ($p > 0.05$) 20 min post-administration of LND and then returned to pretreatment pHi values. Skeletal muscle ($p > 0.05$) and brain ($p = 0.953$) exhibited no significant change in pH_i. We also didn't observe a significant change in pHe of skeletal muscle ($p = 0.312$) or liver ($p = 0.345$) after LND administration, whereas the pHe of brain could not be measured because 3-APP did not cross the blood brain barrier. The bioenergetics of melanoma xenografts and normal tissues were determined from the respective changes in NTP/Pi relative to their baseline levels (Fig. 2D). Evanochko et al. previously reported that the nucleoside triphosphate signal from tumors originates from a mixture of all four nucleotide bases (28), whereas in normal tissues ATP is the predominant nucleotide. As such, values from tumor are represented as NTP and those from brain, liver and muscle are presented as ATP. In tumors the NTP/Pi remained low at 66.8 ± 5.7% ($p < 0.001$) of the baseline level for up to 180 min. However, there was a great range of variability in these 15 measurements (ranging from 6.14 to 77.72%) that went into determining the average change in this ratio. We observed a transient decrease in the liver NTP/Pi while monitoring from baseline ($t = 0$) until $t = 120$ min with a maximum decrease of 32.9 ± 10.6% from the baseline ratio ($p >$

0.05) at t = 40 min. There was no significant change in the bioenergetics of brain ($p > 0.05$) or skeletal muscle ($p > 0.05$).

Steady-state levels of tumor lactate (intracellular plus extracellular) were monitored by ^{1}H MRS with the Had-Sel-MQC pulse sequence. Figure 3 shows representative spectra from one of the three animals that were observed. The integrated intensities of the steady-state lactate peaks relative to the baseline level (as 1.0) were 1.89, 2.27, 3.03, 2.45, 2.30, 2.20, 1.92, 1.79 and 1.52. A U (arbitrary unit) following LND administration at 20, 40, 60, 80, 100, 120, 140, 160 and 180 min, respectively. Lactate intensity peaked at 60 min post LND administration was greater than baseline ($p = 0.009$) integrated intensity and then decreased monotonically (Fig. 2C), (Fig. 3). Note that the decrease in pHi was 0.6 ± 0.1 units, whereas the decrease in pHe was 0.2 ± 0.07 units; since the extracellular volume fraction ranges between about 30 and 50% in experimental tumors (29), this indicates that most of the lactic acid was confined to the intracellular compartment. There was no observed change in tumor pHi, pHe and bioenergetics over a 3 hr period after administration of 3-APP alone (data not shown). ^{31}P MRS demonstrates that the administration of LND increased the pH gradient across the tumor cell membrane: pHe went from 7.00 ± 0.04 to 6.80 ± 0.07 ($p > 0.05$) while pHi went from 6.90 ± 0.05 to 6.33 ± 0.10 ($p < 0.001$).

In preparation for studies combining LND with alkylating agents, we performed *ex vivo* studies of the effects of a number of candidate platinum and alkylating agents on cultured DB-1 melanoma cells. LPAM exhibited the greatest cytotoxicity as a single agent, followed by cisplatin, bendamustine and chlorambucil. LND also exhibited a low level of cytotoxicity as a single agent.

The effects of treatment with LND plus LPAM were evaluated by tumor growth delay experiments (Fig. 4). The effect of treatment with LND + LPAM was significantly different from placebo, LND alone, and LPAM alone ($P < 0.0001$ for all three comparisons).

Tumor growth delay was determined by calculating the time in days between logarithmic regrowth regions of the curves of treated tumors and saline treated controls. Data yielded tumor growth delays in a representative experiment of 1.1 ± 0.1 d, 6.6 ± 0.0 d and 19.9 ± 2.0 d for LND alone, LPAM alone and LND + LPAM, respectively (Fig. 4). Tumor doubling times were estimated from the slopes of the log-linear portion of the tumor regrowth curves determined by linear regression analysis using the formula $Td = 0.3010/m$, where m is the slope. The value of $\log_{10}$ cell-kill, 0.975, estimated from the t = 0 intercept of the plot of log V vs. time, where V = tumor volume, was in excellent agreement with the value obtained from the formula $\log_{10}$ cell kill = $(T-C)/3.32Td = 0.975 \pm 0.110$ (30). Graphical analysis then yields the estimated cell-kill as 89.4 ± 2.2% for LND + LPAM.

Effects of treatment on host body weight reflected overall systemic toxicity. LPAM plus LND, produced a 15.7 ± 3.5% decrease in body weight, but recovery to the control growth rate was complete by 2 wk. The LPAM plus LND results look very encouraging with full recovery of body weight in 14 d and a net tumor growth delay of about 20d.

Discussion

Since the seminal description by Warburg's laboratory that most tumors exhibit high levels of aerobic glycolysis (31, 32), methods have been explored to utilize the "Warburg Effect" for the treatment of cancer, particularly using alkylating agents that are sensitized by acid (10–13) or heat, whose lethal effect is also enhanced under acidic conditions (7–9). Since the MCT is the main mechanism by which the DB-1 melanoma (33) and most other tumors (34) maintain pHi homeostasis, inhibition of this co-transporter would suffice to acidify the tumor.

Spencer and Lehninger (35) first inhibited transport of lactate and pyruvate by administering the MCT inhibitor CHC, which prevented transport of both substituted monocarboxylic acids like lactate and pyruvate but not simple uniacids like acetate or propionate. LND is not as well-documented as an MCT inhibitor, and there have been claims that it was an inhibitor of hexokinase-2 and, hence, glycolysis (36, 37). However, figures 2C and 3 clearly demonstrate that LND increases steady state lactate levels in the tumor by about a factor of three; this was predominantly in the intracellular compartment since pHi decreased much more than pHe. This appears to argue against inhibition of glycolytic metabolism, although other metabolic pathways could also lead to lactic acid production; therefore, quantitative studies of glycolytic pathways will be required to definitively delineate the source of the increased intracellular lactate. Mardor et al. (38) elegantly used diffusion-weighted imaging to demonstrate an increase in intracellular lactate in perfused MCF-7 breast cancer cells following LND treatment. The decrease in pHi induced by LND with minimal change in pHe (Fig. 2) points to the same conclusion as did Ben-Horin et al. (39) on the basis of ^{31}P MRS studies of perfused MCF-7 cells, who also demonstrated by ^{13}C MRS that [2-^{13}C] lactate formed from [1-^{13}C] glucose was retained in the tumor cells after administration of LND. ^{31}P MRS studies by Ben-Yoseph et al. (40) of s.c. 9L glioma tumors in rats confirmed retention of acid under *in vivo* conditions following treatment with LND. Our studies have extended these observations by showing that the effects of LND were restricted to the tumor, by monitoring lactate by ^{1}H MRS *in vivo* and also by showing that lactic acid is retained for at least 3 hr (Fig. 2C), (Fig. 3). This provides a much longer time window for administration of drugs that could be activated by acid than possible with MIBG or CHC alone (~40 min). These extensions beyond the previous studies are critical to ultimate clinical translation.

While LND must be clearly inhibiting export of lactate from the tumor cells of human (DB-1 and MCF-7) and rat origin (9L), it is not clear if it is inhibiting transport of pyruvate into mitochondria as CHC does (35). However, the similar effect of CHC and LND on the bioenergetics of DB-1 melanomas strongly suggests that it is (15).

Therefore, the decline of bioenergetics that was evident both from the decrease in NTP/Pi and from direct monitoring of NTP by ^{31}P MRS vs. time in each animal could be explained by a profound decrease in mitochondrial metabolism following LND administration. This could have been the result of a direct effect of LND on electron transport as Floridi and Lehninger argued on the basis of polarographic data on isolated mitochondria from Ehrlich Ascites cells (41), or it could have been the result of inhibition of pyruvate transport into mitochondria resulting in substrate deprivation for the TCA cycle. The latter explanation is simpler and appears more plausible in view of the demonstration by Spencer and Lehninger (35) that another MCT inhibitor, CHC, blocks transport of both lactate out of the plasma membrane and transport of pyruvate through the mitochondrial membrane.

Overall, our data are fully consistent with the conclusion of Ben-Horin et al. (39) that LND is an inhibitor of the MCT in tumors, thereby impeding export of lactate into the extracellular milieu and accounting for the intracellular acidification induced by LND. If this agent also impedes the transport of pyruvate into mitochondria depriving these organelles of the substrate required for oxidative phosphorylation, the de-energization of the tumor induced by LND would be explained as well. Previously we delivered LND on DB-1 melanomas (15), we delivered the drug i.p. in DMSO solution under hyperglycemic conditions (26 mM blood glucose), maintained by infusion of exogenous glucose. This led to a high level of tumor acidification and de-energization, but the animals used in this preliminary study died. This mortality was completely avoided by eliminating the glucose infusion and by dissolving LND in tris/glycine pH 8.3 buffer before i.p. injection as suggested by Ben-Yoseph et al. (40). This method produced a stable and reproducible

intracellular acidification of the tumor at pHi = 6.33 ± 0.10 over a 3 hr period (Fig. 2) comparable to what had been reported in the previous study by Zhou et al. (15)

Blood tests of mice treated with LND do not indicate any significant renal, bone marrow or hepatic toxicity. Myalgia, and hence muscle toxicity, has been reported in the clinic (42–44). No effect of LND on pHi, pHe or ATP/Pi of muscle was observed in this study (Fig. 2), but it must be remembered that the animals were anesthetized, and hence there was no muscle activity. White muscle fibers are expected to exhibit high levels of glycolytic metabolism during exercise.

We have observed about 30% decrease in the ATP/Pi ratio in DB-1 melanoma xenografts subjected to hyperglycemia and treated with MIBG and CHC (14, 15), and in the current study LND produced a small but transient decrease in liver pHi by 0.2 units and a decrease in ATP/Pi of the liver at 20 min and 40 min, respectively, post-LND administration (Fig. 2). Thus, some liver toxicity may accompany treatment with LND. However, these side effects have not precluded the use of LND in the clinic on over 3500 cancer patients since the early 1980s (H. Seleck, personal communication) and should not prevent the future use in cancer therapy.

As noted above, the activity of platinum compounds and N-mustard alkylating agents (10–13, 16–19) increases with increasing acidification of tumors. In the case of N-mustards, this appears to be due to three effects: 1) increased concentrations of the active intermediate cyclic aziridinium ion intermediate, 2) decreased concentrations of competing nucleophiles such as hydroxide and glutathione, whose production is diminished by decreased activity of gluthathione-S-transferase under acidic conditions, and 3) decreased DNA repair due to acid inhibition of O^6-alkyltransferase (17, 19). This is probably largely because acid shifts the equilibrium between the various forms of these agents towards more active forms. In the case of N-mustards, the active species is the cyclic aziridinium ion. In cells, the reactivity of these agents will also be affected by considerations of transport into the cell and eventually into the nucleus, where DNA alkylation occurs. Sequestration of these agents in lysosomes or other organelles may adversely affect their antineoplastic activity. All these considerations apply to the potential activity of these alkylating agents against melanomas and other tumor cells.

Under neutral conditions such as were utilized in *ex* vivo screening of various alkylating agents, all of the agents should have been able to enter the DB-1 tumor cells. This study indicates that the rank order of reactivity against DB-1 cells of these agents was LPAM > cisplatin > bendamustine > chlorambucil > LND. This makes LPAM an ideal candidate for treatment of DB-1 melanoma xenografts as shown by our previous success with LPAM following acidification in the treatment of melanoma implanted in the hind limb of a rat (16).

In view of this, LPAM seemed to be a good candidate for enhanced activity following DB-1 acidification by LND treatment. LPAM had substantial activity against DB-1 melanoma when administered alone, and this activity was substantially enhanced following the addition of LND, yielding approximately one log order of tumor cell-kill with one treatment. In addition, the animals fully recovered their body weight within about 14 days following treatment with LPAM + LND. Overall, LND + LPAM killed about 90% of the tumor cells. If we waited for about 12 days (i.e., two doubling times) to administer a second dose, the tumor volume should grow back to 40% of its initial volume, and then be diminished again by 90% to 94% of the initial volume since the same dose of drug should produce the same fractional cell kill (45). These results clearly points to a net gain in treatment of DB-1 melanoma with multiple cycles of LPAM + LND. There may be additional beneficial effects

of prolonged and multiple intervals of intracellular acidification associated with inhibition of multidrug resistance (MDR) (46, 47).

LPAM has been used extensively in the clinic in the treatment of multiple myeloma and is known to have considerable bone-marrow toxicity (48). Patients usually require bone marrow transplantation, which has considerable risk of mortality. Other N-mustards such as bendamustine exhibit much lower toxicity (49). This drug and perhaps also cyclophosphamide or other N-mustards may exhibit a better overall therapeutic ratio than LPAM. We plan to explore this possibility in future studies.

In summary, we have achieved our key objective of developing a simple and reproducible procedure for acute intracellular acidification of DB-1 melanomas using the single agent LND, which has been used in clinical treatment of cancer patients for over 30 years. Specifically we have demonstrated that LND-mediates acidification and de-energization selectively in the tumor over a 3 hr period with no effect on muscle or brain and only a much smaller and transient effect on the liver. We demonstrated accumulation of lactate in the tumor by lactate imaging *in vivo* together with measurements of pHi and pHe demonstrating that the acidification was predominantly in the tumor. Increase of the tumor cell membrane pH gradient provides further support for the MCT inhibitor mechanism of LND activity and also suggests that weak bases like doxorubicin should accumulate in melanoma cells after LND administration. We have demonstrated that the effects of 100 mg/kg, i.p. LND without exogenous glucose do not produce mortality and that administration of LND in tris/glycine pH 8.3 buffer avoids mortality even under hyperglycemic conditions. Finally, we showed that LPAM in combination with LND is a good candidate for systemic therapy of melanoma and perhaps other malignancies such as multiple myeloma that are routinely treated with LPAM. Our study provides further support for MCT inhibition being the primary mechanism by which LND modifies intracellular pH and bioenergetics of tumors. Other MCT inhibitors are currently under development by AstraZeneca, Inc. and may exhibit similar properties to LND in modifying tumor pHi and bioenergetics. These agents may, therefore, play an important role in modifying the tumor microenvironment to make cancer more susceptible to certain classes of chemotherapeutic agents and to hyperthermia.

Acknowledgments

We especially thank Drs. Harish Poptani, Sergey Magnitsky, Mohd. Haris, Manoj Kumar and other members of our research group for useful discussion; Brian Weiser and Elliot Woods for their contribution during a Ph.D. rotation and technical position, respectively, in our laboratory. Dr. Saroj P. Mathupala at Wayne State University provided vital insight about the roles of various isoforms of MCT. This study was supported by NIH grants 1-R01-CA-129544-01A2, 5KL2-RR-024132-06, UL1-RR-024134 and utilized the facilities of the Small Animal Imaging Facility and the Abramson Cancer Biostatistics Core Facility of the University of Pennsylvania.

Abbreviations

LND	Lonidamine
LPAM	Melphalan
MRS	Magnetic Resonance Spectroscopy
MCT	Monocarboxylate Transporter
pHi	Intracellular pH
pHe	Extracellular pH
3-APP	3-Aminopropylphosphonate

PME	Phosphomonoester
Pi	Inorganic Phosphate
PDE	Phosphodiester
MIBG	Meta-iodobenzylguanidine
i.p	intraperitoneal
s.c.	Subcutaneous
CHC	α-cyano-4-hydroxycinnamic acid
TCA	tricarboxylic acid

References

1. Jemal A, Siegel R, Ward E, Murray T, Xu JQ, Smigal C, Thun MJ. Cancer statistics, 2006. Ca-a Cancer Journal for Clinicians. Mar-Apr;2006 56(2):106–130. [PubMed: 16514137]
2. American Cancer Society. Cancer Facts and Figures--1994. 1994.
3. Flaherty K, Puzanov I, Sosman J, Kim K, Ribas A, McArthur G, Lee RJ, Grippo JF, Nolop K, Chapman P. Phase I study of PLX4032: Proof of concept for V600E BRAF mutation as a therapeutic target in human cancer. Journal of Clinical Oncology. 2009; 27:9000.
4. Thompson DS, Flaherty K, Messersmith W, Harlacker K, Nallapareddy S, Vincent C, DeMarini DJ, Cox DS, O'Neill VJ, Burris HA. A three-part, phase I, dose-escalation study of GSK1120212, a potent MEK inhibitor, administered orally to subjects with solid tumors or lymphoma. Journal of Clinical Oncology. 2009:27.
5. Hodi FS, O'Day SJ, McDermott DF, Weber RW, Sosman JA, Haanen JB, Gonzalez R, Robert C, Schadendorf D, Hassel JC, Akerley W, van den Eertwegh AJM, Lutzky J, Lorigan P, Vaubel JM, Linette GP, Hogg D, Ottensmeier CH, Lebbe C, Peschel C, Quirt I, Clark JI, Wolchok JD, Weber JS, Tian J, Yellin MJ, Nichol GM, Hoos A, Urba WJ. Improved Survival with Ipilimumab in Patients with Metastatic Melanoma. New England Journal of Medicine. Aug; 363(8):711–723.
6. Thompson JA, Hamid O, Minor D, Amin A, Ron IG, Ridolfi R, Assi H, Berman D, Siegel J, Weber JS. Ipilimumab in Treatment-naive and Previously Treated Patients with Metastatic Melanoma: Retrospective Analysis of Efficacy and Safety Data from a Phase II Trial. Journal of Immunotherapy. Jan; 2012 35(1):73–77. [PubMed: 22130164]
7. Chu GL, Dewey WC. The role of low intracellular or extracellular pH in sensitization to hyperthermic radiosensitization. Radiat Res. Sep; 1988 115(3):576–585. [PubMed: 3174938]
8. Chu GL, Wang ZH, Hyun WC, Pershadsingh HA, Fulwyler MJ, Dewey WC. The role of intracellular pH and its variance in low pH sensitization of killing by hyperthermia. Radiat Res. Jun; 1990 122(3):288–293. [PubMed: 2356282]
9. Lyons JC, Kim GE, Song CW. Modification of intracellular pH and thermosensitivity. Radiat Res. Jan; 1992 129(1):79–87. [PubMed: 1728060]
10. Atema A, Buurman KJ, Noteboom E, Smets LA. Potentiation of DNA-adduct formation and cytotoxicity of platinum-containing drugs by low pH. Int J Cancer. Apr 22; 1993 54(1):166–172. [PubMed: 8478143]
11. Jahde E, Glusenkamp KH, Klunder I, Hulser DF, Tietze LF, Rajewsky MF. Hydrogen ion-mediated enhancement of cytotoxicity of bis-chloroethylating drugs in rat mammary carcinoma cells in vitro. Cancer Res. Jun 1; 1989 49(11):2965–2972. [PubMed: 2720657]
12. Jahde E, Glusenkamp KH, Rajewsky MF. Nigericin enhances mafosfamide cytotoxicity at low extracellular pH. Cancer Chemother Pharmacol. 1991; 27(6):440–444. [PubMed: 2013114]
13. Jahde E, Roszinski S, Volk T, Glusenkamp KH, Wiedemann G, Rajewsky MF. Metabolic response of AH13r rat tumours to cyclophosphamide as monitored by pO2 and pH semi-microelectrodes. Eur J Cancer. 1992; 29A(1):116–122. [PubMed: 1445727]

14. Zhou R, Bansal N, Leeper DB, Glickson JD. Intracellular acidification of human melanoma xenografts by the respiratory inhibitor m-iodobenzylguanidine plus hyperglycemia: A P-31 magnetic resonance spectroscopy study. Cancer Research. Jul; 2000 60(13):3532–3536. [PubMed: 10910065]
15. Zhou R, Bansal N, Leeper DB, Pickup S, Glickson JD. Enhancement of hyperglycemia-induced acidification of human melanoma xenografts with inhibitors of respiration and ion transport. Academic Radiology. Jul; 2001 8(7):571–582. [PubMed: 11450957]
16. Canter RJ, Zhou R, Kesmodel SB, Zhang Y, Heitjan DF, Glickson JD, Leeper DB, Fraker DL. Metaiodobenzylguanidine and hyperglycemia augment tumor response to isolated limb perfusion in a rodent model of human melanoma. Ann Surg Oncol. Mar; 2004 11(3):265–273. [PubMed: 14993021]
17. Kuin A, Aalders M, Lamfers M, van Zuidam DJ, Essers M, Beijnen JH, Smets LA. Potentiation of anti-cancer drug activity at low intratumoral pH induced by the mitochondrial inhibitor m-iodobenzylguanidine (MIBG) and its analogue benzylguanidine (BG). Br J Cancer. Feb; 1999 79(5–6):793–801. [PubMed: 10070871]
18. Skarsgard LD, Skwarchuk MW, Vinczan A, Kristl J, Chaplin DJ. The cytotoxicity of melphalan and its relationship to pH, hypoxia and drug uptake. Anticancer Res. Jan-Feb;1995 15(1):219–223. [PubMed: 7733636]
19. Wong P, Lee C, Tannock IF. Reduction of intracellular pH as a strategy to enhance the pH-dependent cytotoxic effects of melphalan for human breast cancer cells. Clin Cancer Res. May 1; 2005 11(9):3553–3557. [PubMed: 15867259]
20. Hill LL, Korngold R, Jaworsky C, Murphy G, McCue P, Berd D. Growth and metastasis of fresh human melanoma tissue in mice with severe combined immunodeficiency. Cancer Res. Sep 15; 1991 51(18):4937–4941. [PubMed: 1893383]
21. Gillies RJ, Liu Z, Bhujwalla Z. 31P-MRS measurements of extracellular pH of tumors using 3-aminopropylphosphonate. Am J Physiol. Jul; 1994 267(1 Pt 1):C195–203. [PubMed: 8048479]
22. van Sluis R, Bhujwalla ZM, Raghunand N, Ballesteros P, Alvarez J, Cerdan S, Galons JP, Gillies RJ. In vivo imaging of extracellular pH using 1H MRSI. Magn Reson Med. Apr; 1999 41(4):743–750. [PubMed: 10332850]
23. Pickup S, Lee SC, Mancuso A, Glickson JD. Lactate imaging with Hadamard-encoded slice-selective multiple quantum coherence chemical-shift imaging. Magn Reson Med. Aug; 2008 60(2):299–305. [PubMed: 18666110]
24. McCoy CL, Parkins CS, Chaplin DJ, Griffiths JR, Rodrigues LM, Stubbs M. The effect of blood flow modification on intra- and extracellular pH measured by 31P magnetic resonance spectroscopy in murine tumours. Br J Cancer. Oct; 1995 72(4):905–911. [PubMed: 7547238]
25. Seshan, VBN. NMR Spectros-copy Techniques. New York: Marcel Dekker; 1996. In vivo 31P and 23Na NMR spectroscopy and imaging; p. 557-573.
26. Stubbs M, Bhujwalla ZM, Tozer GM, Rodrigues LM, Maxwell RJ, Morgan R, Howe FA, Griffiths JR. An assessment of 31P MRS as a method of measuring pH in rat tumours. NMR Biomed. Nov-Dec;1992 5(6):351–359. [PubMed: 1489671]
27. Diggle, PJ.; Heagerty, P.; Liang, KY.; Zeger, SL. Analysis of Longitudinal Data. 2. 2002.
28. Evanochko WT, Sakai TT, Ng TC, Krishna NR, Kim HD, Zeidler RB, Ghanta VK, Brockman RW, Schiffer LM, Braunschweiger PG, et al. NMR study of in vivo RIF-1 tumors. Analysis of perchloric acid extracts and identification of 1H, 31P and 13C resonances. Biochim Biophys Acta. Sep 14; 1984 805(1):104–116. [PubMed: 6477969]
29. Stubbs M, Rodrigues L, Howe FA, Wang J, Jeong KS, Veech RL, Griffiths JR. Metabolic consequences of a reversed pH gradient in rat tumors. Cancer Res. Aug 1; 1994 54(15):4011–4016. [PubMed: 8033132]
30. Corbett, THaVFA. rodent tumor models in experimental cancer therapy. Kallman, RE., editor. New York: Pergamon Press; 1987.
31. Warburg. The metabolism of tumors. London: Constable and Co; 1930.
32. Weinhouse S. The Warburg hypothesis fifty years later. Z Krebsforsch Klin Onkol Cancer Res Clin Oncol. 1976; 87(2):115–126. [PubMed: 136820]

33. Wahl ML, Owen JA, Burd R, Herlands RA, Nogami SS, Rodeck U, Berd D, Leeper DB, Owen CS. Regulation of intracellular pH in human melanoma: potential therapeutic implications. Mol Cancer Ther. Jun; 2002 1(8):617–628. [PubMed: 12479222]
34. Webb SD, Sherratt JA, Fish RG. Mathematical modelling of tumour acidity: regulation of intracellular pH. J Theor Biol. Jan 21; 1999 196(2):237–250. [PubMed: 9990741]
35. Spencer TL, Lehninger AL. L-lactate transport in Ehrlich ascites-tumour cells. Biochem J. Feb 15; 1976 154(2):405–414. [PubMed: 7237]
36. Floridi A, Bellocci M, Paggi MG, Marcante ML, De Martino C. Changes of energy metabolism in the germ cells and Ehrlich ascites tumor cells. Chemotherapy. 1981; 27(Suppl 2):50–60. [PubMed: 7285638]
37. Floridi A, Paggi MG, D'Atri S, De Martino C, Marcante ML, Silvestrini B, Caputo A. Effect of lonidamine on the energy metabolism of Ehrlich ascites tumor cells. Cancer Res. Nov; 1981 41(11 Pt 1):4661–4666. [PubMed: 7306982]
38. Mardor Y, Kaplan O, Sterin M, Ruiz-Cabello J, Ash E, Roth Y, Ringel I, Cohen JS. Non-invasive real-time monitoring of intracellular cancer cell metabolism and response to lonidamine treatment using diffusion weighted proton magnetic resonance spectroscopy. Cancer Res. Sep 15; 2000 60(18):5179–5186. [PubMed: 11016646]
39. Ben-Horin H, Tassini M, Vivi A, Navon G, Kaplan O. Mechanism of action of the antineoplastic drug lonidamine: 31P and 13C nuclear magnetic resonance studies. Cancer Res. Jul 1; 1995 55(13):2814–2821. [PubMed: 7796408]
40. Ben-Yoseph O, Lyons JC, Song CW, Ross BD. Mechanism of action of lonidamine in the 9L brain tumor model involves inhibition of lactate efflux and intracellular acidification. J Neurooncol. Jan; 1998 36(2):149–157. [PubMed: 9525814]
41. Floridi A, Lehninger AL. Action of the antitumor and antispermatogenic agent lonidamine on electron transport in Ehrlich ascites tumor mitochondria. Arch Biochem Biophys. Oct 1; 1983 226(1):73–83. [PubMed: 6227286]
42. Mansi JL, de Graeff A, Newell DR, Glaholm J, Button D, Leach MO, Payne G, Smith IE. A phase II clinical and pharmacokinetic study of Lonidamine in patients with advanced breast cancer. Br J Cancer. Sep; 1991 64(3):593–597. [PubMed: 1911204]
43. Di Cosimo S, Ferretti G, Papaldo P, Carlini P, Fabi A, Cognetti F. Lonidamine: efficacy and safety in clinical trials for the treatment of solid tumors. Drugs Today (Barc). Mar; 2003 39(3):157–174. [PubMed: 12730701]
44. Roehrborn CG. The development of lonidamine for benign prostatic hyperplasia and other indications. Rev Urol. 2005; 7(Suppl 7):S12–20. [PubMed: 16986056]
45. Skipper HE. On Mathematical-Modeling of Critical Variables in Cancer-Treatment (Goals - Better Understanding of the Past and Better Planning in the Future). Bulletin of Mathematical Biology. 1986; 48(3–4):253–278. [PubMed: 3828557]
46. Simon S, Roy D, Schindler M. Intracellular pH and the control of multidrug resistance. Proc Natl Acad Sci U S A. Feb 1; 1994 91(3):1128–1132. [PubMed: 8302842]
47. Lu Y, Pang T, Wang J, Xiong D, Ma L, Li B, Li Q, Wakabayashi S. Down-regulation of P-glycoprotein expression by sustained intracellular acidification in K562/Dox cells. Biochem Biophys Res Commun. Dec 12; 2008 377(2):441–446. [PubMed: 18851949]
48. Moreau P, Avet-Loiseau H, Harousseau JL, Attal M. Current Trends in Autologous Stem-Cell Transplantation for Myeloma in the Era of Novel Therapies. Journal of Clinical Oncology. May 10; 2011 29(14):1898–1906. [PubMed: 21482979]
49. Ogura M, Uchida T, Taniwaki M, Ando K, Watanabe T, Kasai M, Matsumoto Y, Shimizu D, Ogawa Y, Ohmachi K, Yokoyama H, Tobinai K, Japanese Bendamustine Lymphoma S. Phase I and pharmacokinetic study of bendamustine hydrochloride in relapsed or refractory indolent B-cell non-Hodgkin lymphoma and mantle cell lymphoma. Cancer Science. Sep; 2010 101(9):2054–2058. [PubMed: 20594195]

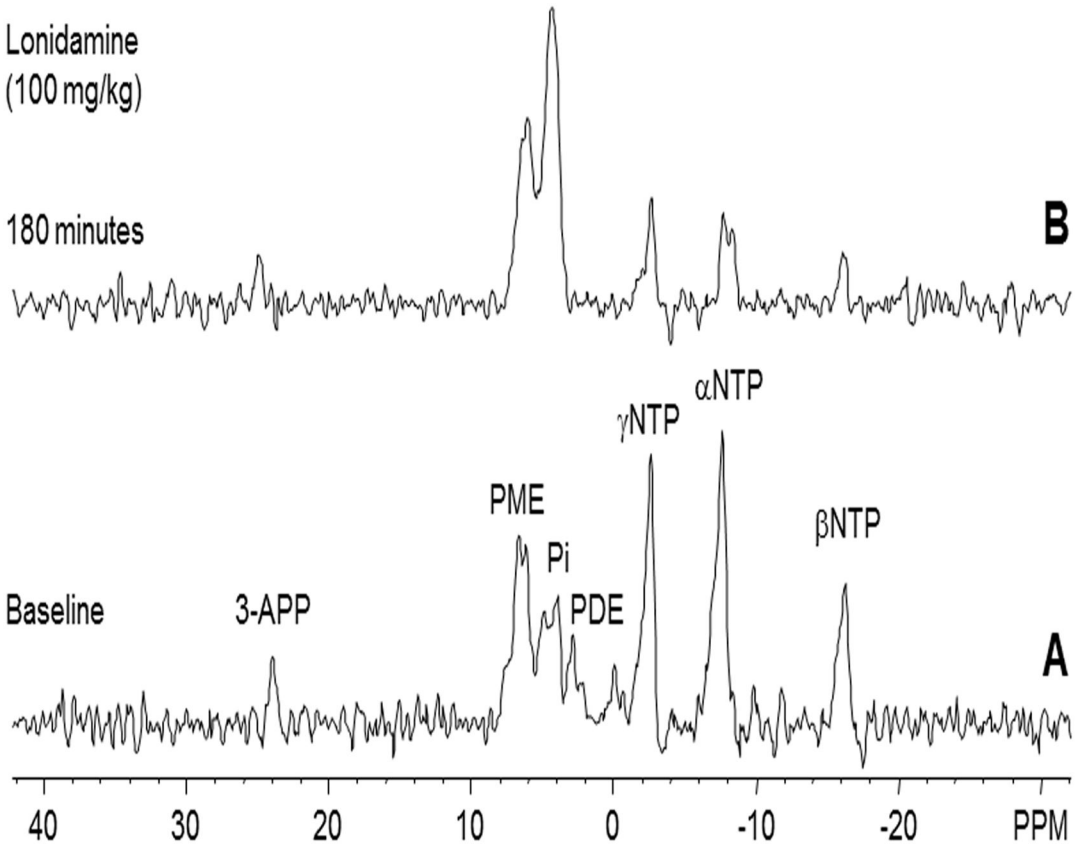

Figure 1.

In vivo localized (Image Selected *In vivo* Spectroscopy - ISIS) ^{31}Phosphorus magnetic resonance spectroscopy (^{31}P MRS) spectra of human melanoma xenograft grown subcutaneously in nude mice (A) pre- and (B) 180 min post administration of LND (100 mg/kg, i.p.). Resonance assignments are as follows, 3-APP (3-aminopropylphosphonate); PME (phosphomonoesters); Pi (inorganic phosphate); PDE (phosphodiesters); γ-NTP (γ-nucleoside-triphosphate), α-NTP (α-nucleoside-triphosphate), β-NTP (β-nucleoside-triphosphate). Decrease in β-NTP levels and the corresponding increase in Pi following LND administration (Spectrum B) indicating impaired energy metabolism.

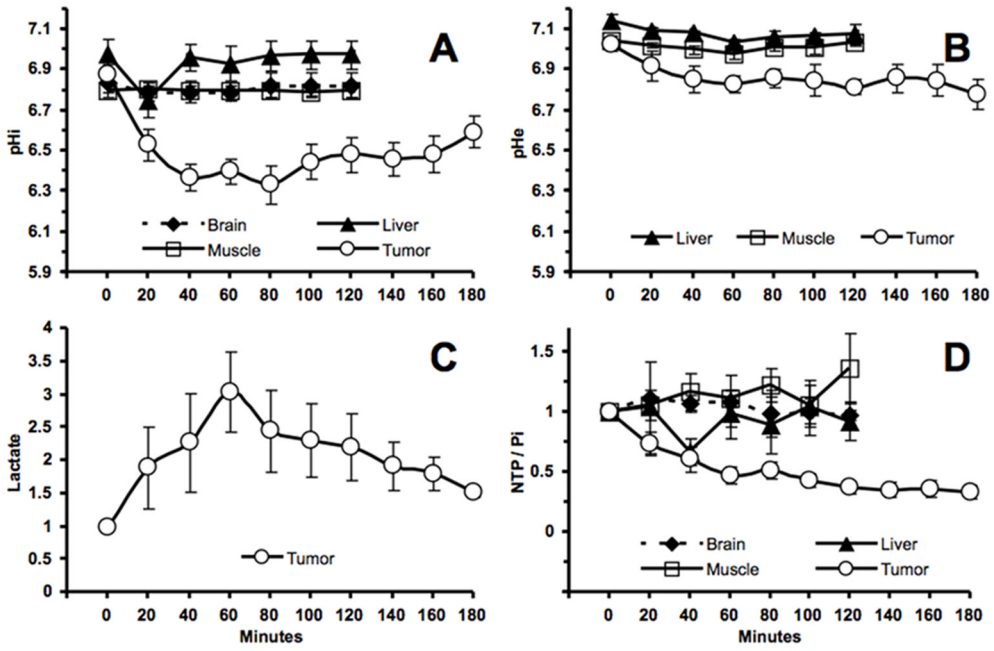

Figure 2.

(A). The intracellular pH (pHi) profile as a function of time of human melanoma xenografts (n = 15) and normal tissues [skeletal muscle (n = 6), liver (n = 6), and brain (n = 3)] in response to LND (100 mg/kg; i.p.) administration at time zero. (B). The extracellular pH (pHe) profile as a function of time of human melanoma xenografts (n = 4) and normal tissues [skeletal muscle (n = 3) and liver (n = 3),] in response to LND (100 mg/kg; i.p.) administration at time zero. (C). Change in tumor lactate as a function of time after administration of LND (100 mg/kg). Area under the curve was compared to baseline at each time points and was normalized to baseline levels. (D). The changes of NTP/Pi (ratio of peak area) relative to baseline as a function of time of human melanoma xenografts (n=15) and normal tissues [skeletal muscle (n = 6), liver (n = 6), and brain (n = 3)] in response to LND (100 mg/kg; i.p.) administration at time zero. The values are presented as mean ± S.E.M. When not displayed, S.E.M. values were smaller than the symbol size.

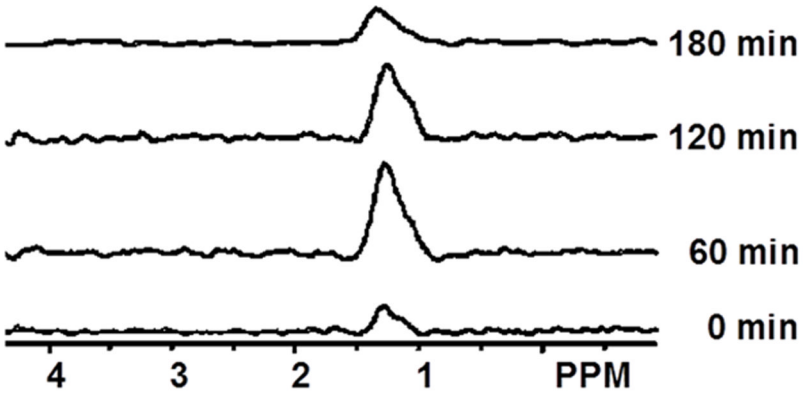

Figure 3.
Spectra show the effect of LND (100 mg/kg) on tumor lactate production. The lactate peak is at 1.3 ppm. Spectra were obtained before any treatment (0 min) and after 60, 120 min and 180 min following LND administration.

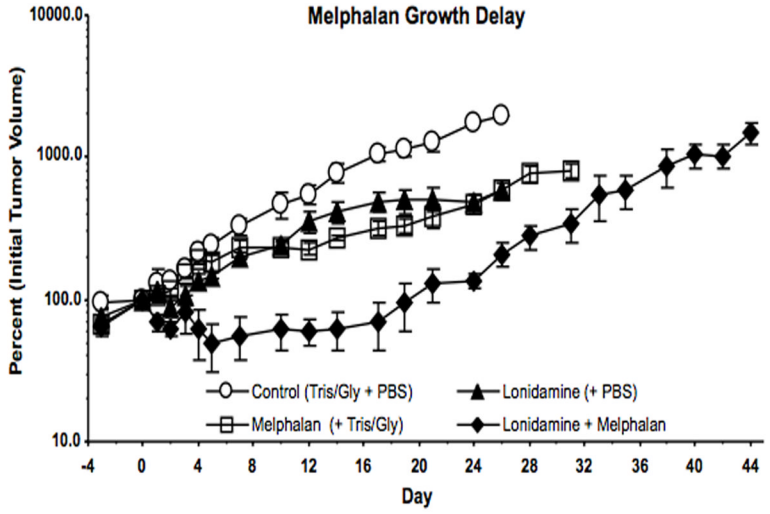

Figure 4.

Growth delay experiments performed on DB-1 human melanoma xenografts in nude mice treated with 7.5 mg/kg LPAM. Mice were treated on Day 0 as follows: Control (sham i.p. tris/glycine buffer + sham i.v. PBS), LND, LPAM, LND + LPAM. Values shown are means ± SEM for n = 4 animals, Control and LND groups; n = 3 animals, LPAM and LND + LPAM groups. When not shown, error bars are less than symbol size.